Manipulation and control of the interfacial polarization in organic light-emitting diodes by dipolar doping

Lars Jäger, Tobias D. Schmidt, Wolfgang Brütting

Angaben zur Veröffentlichung / Publication details:

Jäger, Lars, Tobias D. Schmidt, and Wolfgang Brütting. 2016. "Manipulation and control of the interfacial polarization in organic light-emitting diodes by dipolar doping." *AIP Advances* 6 (9): e095220. https://doi.org/10.1063/1.4963796.

Manipulation and control of the interfacial polarization in organic light-emitting diodes by dipolar doping

Lars Jäger, Tobias D. Schmidt, and Wolfgang Brütting

Citation: AIP Advances **6**, 095220 (2016); doi: 10.1063/1.4963796
View online: https://doi.org/10.1063/1.4963796
View Table of Contents: http://aip.scitation.org/toc/adv/6/9
Published by the American Institute of Physics

Manipulation and control of the interfacial polarization in organic light-emitting diodes by dipolar doping

Lars Jäger,[1,2,a] Tobias D. Schmidt,[1] and Wolfgang Brütting[1,b]
[1]*Institute of Physics, University of Augsburg, 86135 Augsburg, Germany*
[2]*Institute of Materials Resource Management, University of Augsburg, 86135 Augsburg, Germany*

(Received 15 March 2016; accepted 16 September 2016; published online 23 September 2016)

Most of the commonly used electron transporting materials in organic light-emitting diodes exhibit interfacial polarization resulting from partially aligned permanent dipole moments of the molecules. This property modifies the internal electric field distribution of the device and therefore enables an earlier flat band condition for the hole transporting side, leading to improved charge carrier injection. Recently, this phenomenon was studied with regard to different materials and degradation effects, however, so far the influence of dilution has not been investigated. In this paper we focus on dipolar doping of the hole transporting material 4,4-bis[N-(1-naphthyl)-N-phenylamino]-biphenyl (NPB) with the polar electron transporting material tris-(8-hydroxyquinolate) aluminum (Alq_3). Impedance spectroscopy reveals that changes of the hole injection voltage do not scale in a simple linear fashion with the effective thickness of the doped layer. In fact, the measured interfacial polarization reaches a maximum value for a 1:1 blend. Taking the permanent dipole moment of Alq_3 into account, an increasing degree of dipole alignment is found for decreasing Alq_3 concentration. This observation can be explained by the competition between dipole-dipole interactions leading to dimerization and the driving force for vertical orientation of Alq_3 dipoles at the surface of the NPB layer. [http://dx.doi.org/10.1063/1.4963796]

I. INTRODUCTION

Conductivity doping is an established approach to improve charge carrier transport in organic semiconductors.[1–6] Thereby, the carrier density in a doped layer is enhanced by charge transfer between the semiconducting matrix material and the dopant, which is either a strong electron acceptor for p-type or a strong electron donor for n-type doping, respectively. Although the detailed mechanism of the creation of extra charges is still being investigated,[7] this technique is widely used to improve charge injection in optoelectronic devices, like organic light-emitting diodes (OLEDs), or to tune the quasi-Fermi levels in organic solar cells or transistors.[8]

An alternative way to modify charge injection behavior in organic heterojunction devices makes use of interfacial polarization caused by partial alignment of the permanent dipole moments of polar molecules. In OLEDs this offers the possibility of enhancing device performance by tuning the electric field distribution inside the device. In this context, tris-(8-hydroxyquinolate) aluminum (Alq_3), see fig. S1 in supplementary material, served as prototypical material. Berleb *et al.*[9] performed the first measurements on bilayer OLEDs comprising 4,4-bis[N-(1-naphthyl)-N-phenylamino]-biphenyl (NPB) as well as Alq_3 and observed an increasing mismatch between the hole injection voltage (V_t) and the built-in voltage (V_{bi}), for which bipolar charge

[a]Electronic mail: lars.jaeger@physik.uni-augsburg.de
[b]Electronic mail: wolfgang.bruetting@physik.uni-augsburg.de

carrier transport takes place, with increasing Alq_3 thickness. They explained this behavior with a fixed amount of negative charges at the NPB/Alq_3 interface. Ito *et al.*[10] found that polarization not only exists at the interface to the hole transport layer but prevails throughout the whole Alq_3 layer and leads to a giant surface potential (GSP) – in this case with positive sign – at the top. Meanwhile, it has been shown that a variety of polar materials, like 1,3,5-tris(1-phenyl-1 H-benzimidazol-2-yl)benzene (TPBi), 2,9-dimethyl-4,7-diphenyl-1,10-phenanthroline (BCP) and 1,3-bis[2-(4-tert-butylphenyl)-1,3,4-oxadiazo-5-yl]benzene (OXD-7), intrinsically exhibit this behavior.[11] It was also demonstrated that it can serve as a very sensitive probe for OLED degradation.[12–15]

However, while interfacial polarization is well investigated in neat materials, there is a lack of publications evaluating the behavior for two-component diluted systems. Hence, a closer look at guest-host systems with varying concentrations of a polar species in a non-polar matrix — dipolar doping so to say — could lead to a better understanding of molecular interactions leading to a net orientation of the permanent dipole moments.

In this study, we performed impedance spectroscopy for bilayer devices consisting of NPB as hole transport layer (HTL) and a blend of NPB:Alq_3 as electron transport layer (ETL). A comparison to neat Alq_3 films in bi-layered OLEDs reveals deviations from the expected behavior, which would be a linear correlation between the amount of Alq_3 and the magnitude of interfacial polarization. Indeed, the interfacial charge density does not scale linearly with the effective Alq_3 thickness but reaches a maximum for a 1:1 blend. By simple calculations considering the magnitude of the permanent dipole moment and the packing density of Alq_3 molecules, a steadily increasing (normalized) fraction of vertically aligned Alq_3 molecules can be found for a decreasing doping concentration of the polar material.

II. EXPERIMENTAL

The investigated devices (see fig. 1) consist of a semitransparent indium tin oxide (ITO) anode on a glass substrate, followed by Dipyrazino[2,3-f :2',3'-h]quinoxaline-2,3,6,7,10,11-hexacarbonitrile (HATCN) as a hole generation layer. As hole transport layer 60 nm of NPB is used. The electron transporting layer is a blend consisting of NPB and the polar material Alq_3. Finally a 15 nm thick calcium layer is covered with 100 nm aluminum forming the cathode. The thickness of the ETL blend is varied for different mixing ratios and lies between 60 and 140 nm. Details about sample fabrication can be found in the supplementary material.

Devices were electrically characterized by current density-voltage-luminance measurements and impedance spectroscopy. The former are not shown here because there is no important contribution. For the latter we used a Solartron Impedance Analyzer SI 1260 combined with a Dielectric Interface SI 1296. The AC voltage level was 100 mV (r.m.s.). A detailed description of the analysis method can be found, e.g., in the publications by Nowy *et al.*[12] and Schmidt *et al.*[16]

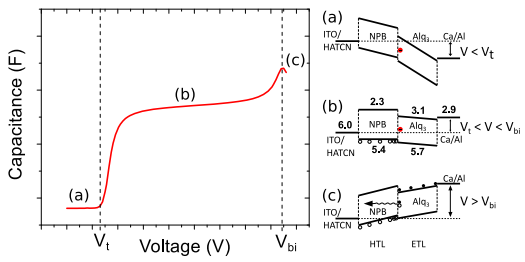

FIG. 1. Capacitance-voltage plot (left) and band diagrams (right) for a two-layered OLED. The labels (a) – (c) of the band diagrams correspond to the different voltages indicated in the $C - V$ plot. The energies of the highest occupied molecular orbital (HOMO) and the lowest unoccupied molecular orbital (LUMO) of the organic materials together with the work functions of the contacts — all given in eV — are indicated in band diagram (b) and come from refs. 17–19.

III. RESULTS AND DISCUSSION

In an electrical impedance measurement a small alternating AC voltage, usually super-imposed on a constant DC bias, is applied to the sample. The measured response is an alternating current with a possible phase shift between voltage and current. The complex impedance Z is defined as the ratio between AC voltage and current. The relevant representation of the complex impedance in the context of this work is the total device capacitance C, which is given by:

$$C = -\frac{1}{2\pi f}\frac{\mathrm{Im}(Z)}{|Z|^2}, \tag{1}$$

with f being the measurement frequency. In the following, the measured data is depicted in terms of capacitance-voltage ($C-V$) plots, with V denoting the applied DC bias.

The investigated OLEDs consist of two layers contributing to the impedance, HTL and ETL, while the HATCN layer only serves as a hole generation layer. Hence, a two layered OLED with a polar ETL leads to a characteristic $C-V$ behavior shown in fig. 1. For voltages lower than the hole injection voltage V_t, region (a), no charge carrier injection occurs and the measured capacitance is equal to the geometric device capacitance with a dielectric constant ϵ_r between the electrodes. Due to the negative interfacial charge the flat band condition for the HTL and with it, the hole injection takes place before electron injection is present. Therefore, above V_t in region (b) holes accumulate at the HTL/ETL interface and the capacitance is given by the ETL thickness. For voltages higher than the built-in voltage V_bi, region (c), both hole and electron injection are possible and, as a consequence, exciton formation and light emission are observed. This leads initially to a strong increase and a subsequent drop of the capacitance.

Fig. 2 shows the results of the interfacial charge density σ_if for different Alq_3 concentrations in the electron transporting layer. The values were calculated with equation 2 introduced by Brütting *et al.*:[20]

$$\sigma_\mathrm{if} = \frac{\epsilon_0\epsilon_\mathrm{r}}{d_\mathrm{ETL}}(V_\mathrm{t}-V_\mathrm{bi}) = \frac{C_\mathrm{ETL}}{A}(V_\mathrm{t}-V_\mathrm{bi}) \tag{2}$$

Here d_ETL and C_ETL are the thickness and capacitance of the electron transporting layer, respectively, and A is the pixel area. As mentioned before, V_t and V_bi do not coincide for polar materials, which is the manifestation of interfacial polarization. The values to calculate σ_if were extracted from $C-V$ measurements depicted in the inset of fig. 2 and the supplementary material. Additionally the varying plateau heights can be linked to the varying layer thicknesses of the ETL. Hence, the $C-V$ measurements clearly demonstrate that hole injection takes place before electron injection sets in. Therefore the ETL has to contain the polar species and Alq_3 can be identified due to the fact that NPB has no permanent dipole moment. Furthermore, we do not observe a shift of the built-in voltage upon mixing of Alq_3 and NPB in the ETL. Hence, although a two-peaked density of LUMO states

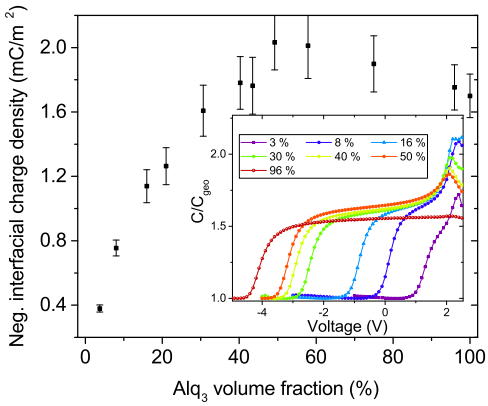

FIG. 2. Calculated interfacial charge densities for the different Alq_3 volume fractions in the ETL. Here 0 % implies a neat NPB layer as ETL and 100 % a neat Alq_3 layer. In contrast to the expectation the polarization reaches a maximum for a 1:1 mixture. The inset shows exemplarily $C-V$ measurements. The complete set of $C-V$ data and the corresponding device parameters can be found in fig. S2 and tab. SI of the supplementary material.

is present in the blend, interfacial charge equilibration[21] leading to a modification of the effective cathode work function does not seem to play a prominent role in these devices.

In fig. 2 the global maximum of the (negative) interfacial charge density is found for an Alq_3:NPB mixing ratio of 1:1 with a magnitude of about 2.0 mC/m^2. Normally one would expect the highest value for a neat Alq_3 layer and the polarization should scale linearly with the doping concentration and vanish for the neat, non-polar NPB case. By contrast, starting at 1.7 mC/m^2 in neat Alq_3 there is a slight increase to 2.0 mC/m^2 for 50 % doping. However, for further lowering the Alq_3 content a strong decrease of the polarization takes place resulting in a remaining interface charge density of 0.37 mC/m^2 for a blend with 3.75 % Alq_3, only.

Taking the permanent dipole moment of Alq_3, μ = 3.9 D,[22,23] together with the volume per molecule into account, the maximum possible polarization can be calculated according to:

$$\sigma_{\mathrm{if}}^{\mathrm{max}} = \frac{\mu}{V}. \tag{3}$$

Using crystallographic data for the α-phase of Alq_3 with a unit cell volume of 1111 Å^3 (comprising 2 molecules)[24,25] and assuming 75 % space filling, a value of $\sigma_{\mathrm{if}}^{\mathrm{max}} \approx 20$ mC/m^2 is obtained. This, however, implies a sheet of Alq_3 molecules with all dipole moments perfectly aligned in the direction of the substrate normal. Comparing this value to the experimentally measured interface charge density for a neat Alq_3 film leads to the conclusion that only about 10 % of all molecules effectively contribute to the net orientation, while the other 90 % somehow neutralize each other. Furthermore, by simply dividing the interfacial charge density by the known doping concentration, one can determine a normalized quantity, which corresponds to the fraction of vertically aligned Alq_3 molecules that are required to account for the interfacial polarization in the blends.

Fig. 3 illustrates this number for the different doping concentrations. Again, a priori one would expect a constant line at around 10 %. Instead, starting at 10 % for the neat Alq_3 layer a steady increase is observed reaching about 60 % for the lowest investigated doping concentration. This implies a six times higher effective contribution of the Alq_3 molecules at low doping. Values for even lower doping concentrations are hard to obtain due to the fact that the plateau in the capacitance-voltage sweep is no longer resolvable.

Considering the polarization effect of a neat Alq_3 layer we assume that there could be two reasons for this phenomenon. On the one hand, the interfacial charge could arise from a small deviation from a perfectly isotropic orientation distribution of the molecules. On the other hand, which we think is more likely, the effect could be ascribed to the formation of Alq_3 pairs of anti-parallel dipole alignment, like in a crystalline unit cell,[25] with a small fraction of unpaired dipole moments remaining in the film.

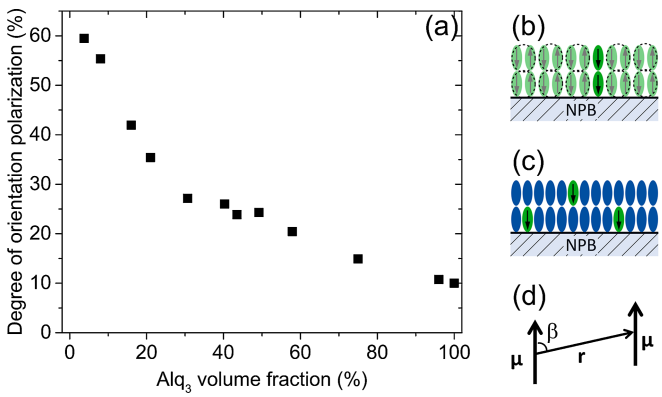

FIG. 3. (a) Calculated degree of orientation polarization. A steady increase between the Alq_3 volume fraction and the percentage of contributing molecules is observed. In the case of a 3.75 % dilution there is a six times higher alignment compared to the starting value of a neat Alq_3 film. The sketches (b) and (c) illustrate the behavior for high and low Alq_3 content in the mixture, respectively. The green ellipses are the Alq_3 molecules and the blue ellipses are NPB molecules. Sketch (d) shows the situation for two parallel interacting dipole moments with the parameters used in equation 4.

This behavior can be further justified by the calculations of Noguchi *et al.*[11,26] of the potential energy for two permanent dipoles with either parallel or antiparallel alignment:

$$U_{\uparrow\uparrow} = -\frac{1}{4\pi\varepsilon_0}\frac{\mu^2}{r^3}(3\cos^2\beta - 1) \quad \text{and} \quad U_{\uparrow\downarrow} = -U_{\uparrow\uparrow} \tag{4}$$

Therein μ is the magnitude of the permanent dipole moment of each molecule, r is the distance between the centers of the dipoles and β the angle between the direction of the dipoles and the line connecting their centers (see sketch in fig. 3(d)). Given the fact that the considered dipole orientations here are along the surface normal of the glass substrate, this expression immediately leads to two possible configurations with local energy minima. For molecules in the substrate plane ($\beta = 90°$) anti-parallel alignment is preferred, while parallel alignment is energetically favorable for stacked molecules out of plane ($\beta = 0°$). This means that once a certain amount of molecules with unpaired dipoles exists in the first monolayer on a substrate, this state with "broken symmetry" will persist throughout the whole film.

Obviously, since Alq_3 films are known to be amorphous – or at best nanocrystalline – not all of the molecular dipole moments are paired leaving some molecules to built up a net polarization. The observation of growing polarization with reduced Alq_3 content in the ETL can now be rationalized by two complementary effects, namely an attenuated dipole-dipole interaction with increasing intermolecular distance and an interaction of Alq_3 molecules with the surface of NPB leading to a preferred vertical orientation of their dipole moments.

In the lowest dilution the Alq_3 molecules are more or less isolated from each other, because the average distance between neighboring Alq_3 molecules is 27.6 Å compared to 9.2 Å in a neat Alq_3 layer. This can be calculated from the unit cell[27] and the assumption of a close-packing of spheres. As a consequence, the interaction potential ($\propto r^{-3}$) is smaller by almost a factor of 30. Thus, the growth condition is dominated by the interaction between NPB and Alq_3. Thereby, electrostatic as well as steric mechanisms could play a role. Molecular electrostatic potential calculations of NPB[28] reveal an almost completely electropositive surface so that a preferential growth orientation may exist, where the permanent dipole moment of Alq_3 is pointing towards the NPB surface. To fully explain the behavior, however, molecular dynamics simulations taking interface energetics into account are necessary, which would go far beyond the scope of this letter.

With increasing Alq_3 content in the blend the distance between neighboring Alq_3 molecules decreases. Hence, the dipole-dipole interaction becomes larger and the probability of forming aggregates with anti-parallel aligned permanent dipole moments increases. Additionally the temperature of the substrate (here: room temperature) as well as the glass transition temperature of the mixture[29] can have an impact on orientation. Recently several publications[30–32] show a pronounced molecular orientation for a low substrate temperature compared to the glass transition temperature T_g of the evaporated organic layer. Alq_3 has a high glass transition of $T_g(Alq_3) = 175$ °C,[29] while NPB with only $T_g = 98$ °C[33] is much lower. Thus, the overall glass transition temperature of the blend is continuously increasing with the Alq_3 amount and reaches its highest value for the neat Alq_3 film.[34] Therewith, the reduced molecular motion at the surface of the growing film with increasing Alq_3 content could prevent Alq_3 molecules from fully equilibrating toward the energetically favored anti-parallel alignment.

Taking all the mentioned effects together, there is a steady development from parallel aligned permanent dipole moments for the highly diluted blend to more and more anti-parallel aligned permanent dipole moments with increasing Alq_3 content. However, even in the neat Alq_3 film a net polarization corresponding to 10% aligned molecules remains.

IV. CONCLUSION

Impedance spectroscopy is a powerful tool to investigate polarization effects in organic heterolayer devices. In this paper we performed measurements on simple OLED stacks comprising a mixture of the nonpolar hole transporting material NPB and the polar electron transporting material Alq_3. By extracting the interfacial charge density, obtained from C-V measurements, we obtained a nonlinear relationship between the Alq_3 volume fraction and the interfacial charge density.

Surprisingly, a maximum of the polarization for a 1:1 dilution was found. By simple calculations we trace this effect back to an increasing net orientation of the permanent dipole moments of Alq_3. As tentative explanation we suggest a subtle interplay of competing interactions, namely an electrostatic interaction between the surface of NPB and Alq_3 molecules acting toward parallel alignment of their dipoles and the effect of an increasing dipole-dipole interaction with growing Alq_3 content favoring anti-parallel alignment. Furthermore, since the glass transition temperature of the blend changes considerably with composition, a kinetic influence of the orientation dynamics at the surface of the growing film is very likely. Molecular dynamics simulations of the growth of such blend layers could give further insights into these issues. Moreover, as many organic semiconductors have permanent dipole moments, for future optimization of OLEDs in terms of efficiency and long-term stability, it is crucial to take changes of the polarization into account. This effect manipulates the internal electric field distribution and enables an alternative way to control charge injection and accumulation behavior in optoelectronic devices.

SUPPLEMENTARY MATERIAL

See supplementary material for molecular structure of Alq_3, a detailed description of device fabrication and the complete data set of $C - V$ measurements.

ACKNOWLEDGMENTS

The authors would like to acknowledge financial support by the German Research Foundation (DFG) within the project "CARDYN" (contract no.: BR 1728/15-1) and the German Federal Ministry of Education and Research (BMBF) within the "Interphase" project (contract no. 13N13664). L.J. also acknowledges a PhD scholarship by the Bavarian State Ministry of Education and Culture, Science and the Arts as part of the Graduate School "Ressourcenstrategische Konzepte für zukunftsfähige Energiesysteme".

[1] C.-C. Chang, M.-T. Hsieh, J.-F. Chen, S.-W. Hwang, and C. H. Chen, Appl. Phys. Lett. **89**, 253504 (2006).
[2] B. Lüssem, M. Riede, and K. Leo, Phys. Status Solidi A **210**, 9 (2013).
[3] M. Pfeiffer, K. Leo, X. Zhou, J. S. Huang, M. Hofmann, A. Werner, and J. Blochwitz-Nimoth, Org. Electron. **4**, 89 (2003).
[4] J. T. Lim, K. N. Kim, and G. Y. Yeom, J. Nanosci. Nanotechnol. **9**, 7485 (2009).
[5] H. X. Wei, Q.-D. Ou, Z. Zhang, J. Li, Y.-Q. Li, S.-T. Lee, and J.-X. Tang, Org. Electron. **14**, 839 (2013).
[6] D.-S. Leem, H.-D. Park, J.-W. Kang, J.-H. Lee, J. W. Kim, and J.-J. Kim, Appl. Phys. Lett. **91**, 011113 (2007).
[7] H. Méndez, G. Heimel, S. Winkler, J. Frisch, A. Opitz, K. Sauer, B. Wegner, M. Oehzelt, C. Röthel, S. Duhm, D. Többens, N. Koch, and I. Salzmann, Nat. Commun. **6**, 8560 (2015).
[8] B. Lüssem, M. L. Tietze, H. Kleemann, J. W. Hobach, C. Bartha, A. Zakhidov, and K. Leo, Nat. Commun. **4**, 2775 (2013).
[9] S. Berleb, W. Brütting, and G. Paasch, Org. Electron. **1**, 41 (2000).
[10] E. Ito, Y. Washizu, N. Hayashi, H. Ishii, N. Matsuie, K. Tsuboi, Y. Ouchi, Y. Harima, K. Yamashita, and K. Seki, J. Appl. Phys. **92**, 7306 (2002).
[11] Y. Noguchi, Y. Miyazaki, Y. Tanaka, N. Sato, Y. Nakayama, T. D. Schmidt, W. Brütting, and H. Ishii, J. Appl. Phys. **111**, 114508 (2012).
[12] S. Nowy, W. Ren, A. Elschner, W. Lövenich, and W. Brütting, J. Appl. Phys. **107**, 054501 (2010).
[13] D. Y. Kondakov, J. R. Sandifer, C. W. Tang, and R. H. Young, J. Appl. Phys. **93**, 1108 (2003).
[14] H. Aziz, Z. D. Popovic, N.-X. Hu, A.-M. Hor, and G. Xu, Science **283**, 1900 (1999).
[15] D. Y. Kondakov and R. H. Young, J. Appl. Phys. **108**, 074513 (2010).
[16] T. D. Schmidt, L. Jäger, Y. Noguchi, H. Ishii, and W. Brütting, J. Appl. Phys. **117**, 215502 (2015).
[17] A. Buckley, *Organic Light-Emitting Diodes (OLEDs): Materials, Devices and Applications*, 1st ed. (Woodhead Publishing, 2013), ISBN: 978-0-85709-894-8.
[18] S. Lee, J.-H. Lee, J.-H. Lee, and J.-J. Kim, Adv. Funct. Mater. **22**(4), 855 (2012).
[19] T. Tsuboi, T. Kishimoto, K. Wako, K. Matsuda, and H. Iguchi, Phys. Status Solidi A **8**(9), 2903 (2011).
[20] W. Brütting, S. Berleb, and A. G. Mückl, Org. Electron. **2**, 1 (2001).
[21] M. Oehzelt, N. Koch, and G. Heimel, Nat. Commun. **5**, 4174 (2014).
[22] A. Curioni, M. Boero, and W. Andreoni, Chem. Phys. Lett. **294**, 263 (1998).
[23] S. Yanagisawa and Y. Morikawa, Jpn. J. Appl. Phys. **45**, 413 (2006).
[24] M. Braun, J. Gmeiner, M. Tzolov, M. Cölle, F. D. Meyer, W. Milius, H. Hillebrecht, O. Wendland, J. U. von Schütz, and W. Brütting, J. Chem. Phys. **114**, 9625 (2001).
[25] M. Brinkmann, G. Gadret, M. Muccini, C. Taliani, N. Masciocchi, and A. Sironi, J. Am. Chem. Soc. **122**, 5147 (2000).
[26] W. Brütting and C. Adachi, *Physics of Organic Semiconductors*, 2nd ed. (Wiley-VCH Verlag GmbH & Co. KGaA, 2012), ISBN: 978-3-527-41053-8.
[27] M. Cölle and W. Brütting, Phys. Status Solidi A **201**, 1095 (2004).

[28] K.-H. Kim, S. Lee, C.-K. Moon, S.-Y. Kim, Y.-S. Park, J.-H. Lee, J.-W. Lee, J. Huh, Y. You, and J.-J. Kim, Nat. Commun. **5**, 4769 (2014).
[29] C. Mayr and W. Brütting, Chem. Mater. **27**, 2759 (2015).
[30] D. Yokoyama, J. Mater. Chem. **21**, 19187 (2011).
[31] S. S. Dalal, D. M. Walters, I. Lyubimov, J. J. de Pablo, and M. D. Ediger, PNAS **112**, 4227 (2015).
[32] I. Lyubimov, L. Antony, D. M. Walters, D. Rodney, M. D. Ediger, and J. J. de Pablo, J. Chem. Phys. **143**, 094502 (2015).
[33] Q.-X. Tong, S.-L. Lai, M.-Y. Chan, K.-H. Lai, J.-X. Tang, H.-L. Kwong, C.-S. Lee, and S.-T. Lee, Chem. Mater. **19**, 5851 (2007).
[34] J. Jiang, D. M. Walters, D. Zhou, and M. D. Ediger, Soft Matter **12**, 3265 (2016).